Atmospheric dynamics feedback: concept, simulations and climate implications

Michael P. Byrne*

ETH Zürich, Zürich, Switzerland

Tapio Schneider

California Institute of Technology, Pasadena, California

Corresponding author address: Michael P. Byrne, Institute for Atmospheric and Climate Science, Universitätstrasse 16, 8092 Zürich, Switzerland

E-mail: michael.byrne@erdw.ethz.ch

ABSTRACT

The regional climate response to radiative forcing is largely controlled by changes in the atmospheric circulation. It has also been suggested that global climate sensitivity depends on the circulation response, an effect we call the "atmospheric dynamics feedback". Using a technique to isolate the effect of changes in atmospheric circulation on top-of-atmosphere (TOA) radiation, we calculate the atmospheric dynamics feedback in coupled climate models. Large-scale circulation changes shape clear-sky and particularly cloud feedbacks in the tropics but are relatively less important at higher latitudes. Globally averaged, the dynamics feedback is small and positive and contributes to model uncertainty in the near-surface temperature response to climate change. A fundamental constraint related to the atmospheric mass budget results in the global dynamics feedback being negligible relative to feedbacks associated with thermodynamic processes. Idealized forcing simulations suggest that circulation changes at high latitudes are more effective at influencing global temperature than circulation changes at low latitudes, and the implications for past and future climate change are discussed.

1. Introduction

The general circulation of the atmosphere is expected to change in a variety of ways as the climate warms in response to CO_2-induced radiative forcing. Projected circulation responses include a widening of the Hadley circulation (Lu et al. 2007), a narrowing of the intertropical convergence zone (ITCZ) (Byrne and Schneider 2016b), a slowdown in the Walker circulation (Vecchi and Soden 2007), and a poleward shift of the mid-latitude storm tracks (Yin 2005; O'Gorman 2010; Chang et al. 2012; Shaw et al. 2016; Mbengue and Schneider 2017). Regional climate change, including projected changes in the water cycle, is strongly dependent on these circulation responses (e.g., Seager et al. 2010; Scheff and Frierson 2012; Shepherd 2014; Byrne and O'Gorman 2015; Byrne and Schneider 2016b). Not only does the circulation response affect regional climate but it has also been suggested that global climate change may be amplified or dampened by the atmospheric circulation response. We refer to this effect as the "atmospheric dynamics feedback".

Studies of how the atmospheric circulation response to global warming affects the top-of-atmosphere (TOA) radiative balance and climate change have largely focused on interactions between the tropical circulation and clouds (Lindzen et al. 2001; Bony et al. 2004; Mauritsen and Stevens 2015). The "iris" hypothesis of Lindzen et al. (2001) suggested that a decrease in the portion of the tropics covered by high convective clouds and a concurrent increase in low-cloud area under global warming is an important negative feedback on climate change. Pierrehumbert (1995) put forward a similar mechanism to explain the stability of warm climates in the past (e.g., the Eocene). The physics of this proposed feedback are intuitive and rely on differences in cloud radiative effect (CRE) between low-cloud and high-cloud regions[1]. Low clouds have a negative

[1]The shortwave and longwave cloud radiative effects are defined conventionally as the differences between the all-sky outgoing shortwave or longwave fluxes at TOA and the clear-sky fluxes (Allan 2011): $CRE^{\mathrm{SW}} = SW^{\mathrm{TOA}}_{\mathrm{clear}} \uparrow - SW^{\mathrm{TOA}}_{\mathrm{all}} \uparrow$ and $CRE^{\mathrm{LW}} = LW^{\mathrm{TOA}}_{\mathrm{clear}} \uparrow - LW^{\mathrm{TOA}}_{\mathrm{all}} \uparrow$, where $\uparrow$ denotes an upward flux. The shortwave and longwave clear-sky radiative effects are defined as: $CSRE^{\mathrm{SW}} = SW^{\mathrm{TOA}}_{\mathrm{clear}} \uparrow$ and $CSRE^{\mathrm{LW}} = LW^{\mathrm{TOA}}_{\mathrm{clear}} \uparrow$

CRE and cool the Earth because they reflect shortwave radiation yet have only a weak longwave greenhouse warming effect because they exist close to the Earth's surface. High clouds, on the other hand, have a CRE that is close to zero because of the large cancellation between shortwave cooling and longwave warming (Ramanathan et al. 1989). Consequently, a decrease in the area of neutral high clouds and an increase in the area of cooling low clouds under global warming is a possible negative climate feedback.

Although the validity of the iris hypothesis proposed by Lindzen et al. (2001) has been strongly challenged (e.g., Fu et al. 2002), recent studies have revived interest in iris-type phenomena as potentially important negative feedbacks on climate change (Mauritsen and Stevens 2015; Bony et al. 2016). The suggestion that tropical convection will become more aggregated as sea-surface temperatures increase (e.g., Wing and Emanuel 2014) has formed the conceptual basis for these 'iris 2.0' studies. Convective aggregation is not typically simulated by global climate models, in which convection is parameterized out of necessity, but it has been put forward as an iris-type atmospheric dynamics feedback (Wing et al. 2017). Perhaps related to convective aggregation, a narrowing of tropical high-cloud regions (i.e., the ITCZ) relative to low-cloud regions with global warming has been observed over recent decades (Wodzicki and Rapp 2016), and the ITCZ is expected to narrow further as the climate continues to warm (Byrne and Schneider 2016b) – ITCZ narrowing represents another potential iris effect. At higher latitudes, cloud feedbacks associated with shifts in the extratropical atmospheric circulation have also received considerable attention in recent years (Grise et al. 2013; Kay et al. 2014; Wall and Hartmann 2015), though climate models disagree on the magnitude and importance of this feedback (Ceppi et al. 2017).

The studies mentioned above focus on cloud feedbacks, but it is plausible that a re-organization of the atmospheric circulation could also affect the water vapor feedback by changing the spatial patterns and intensities of moisture convergence and divergence zones. More generally, atmo-

spheric circulation changes can influence both the CRE, the clear-sky radiative effect (CSRE), and the all-sky radiative effect (ASRE) at all latitudes[1], but the magnitudes of these atmospheric dynamics feedbacks and their dependences on latitude are unknown. Are there latitudes at which climate feedbacks are dominated by large-scale circulation changes? How do circulation changes in general contribute to global climate change? Can an understanding of atmospheric dynamics in a changing climate help to better constrain global climate sensitivity? Are low-latitude or high-latitude circulation changes more effective at changing global temperature? A number of studies have shown that the spatial pattern of ocean heat uptake strongly affects the global temperature response (Rose et al. 2014; Rugenstein et al. 2016), i.e., heat absorbed by the ocean at high latitudes has a much stronger effect on global temperature than the same quantity of heat absorbed at low latitudes. Should such a latitudinal dependence also exist for the atmospheric dynamics feedback, it would have important implications for the ability of tropical iris-type mechanisms to regulate past and future climate change.

Here we use coupled climate models together with idealized forcing simulations to assess how the large-scale atmospheric circulation contributes to TOA radiative anomalies and global climate change. We begin by outlining the method used to decompose dynamic vs thermodynamic influences on TOA radiation (section 2) before analysing the atmospheric dynamics feedback in simulations with coupled models (section 3). Idealized simulations with a range of stylized TOA forcings are also performed to understand how circulation changes at different latitudes could influence global climate (section 4). We conclude by summarizing our results and discussing outstanding questions and directions for future research (section 5).

2. Estimating the atmospheric dynamics feedback

We use a modified version of the method of Bony et al. (2004) to decompose changes in TOA radiation into dynamic, thermodynamic, and nonlinear components (where nonlinear here represents the combined influence of changes in dynamic and thermodynamic processes on TOA radiation). The Bony et al. (2004) method assumes that, to first order, CRE is controlled by the mid-tropospheric vertical velocity, ω. We extend this method and further assume a strong control of ω on CSRE and ASRE. To estimate how changes in the large-scale atmospheric circulation affect TOA radiation, we first construct discretized functions $R(\omega)$ for a defined region, where R is either the area-weighted CRE, CSRE or ASRE 'binned' as a function of mid-tropospheric vertical velocity. We also construct normalized area probability density functions (PDFs) for vertical velocity in the defined region, $A(\omega)$. In this framework, the average CRE, CSRE or ASRE ($\overline{R}$) in the region is the product of $R(\omega)$ and $A(\omega)$ summed over all ω bins, which in continuous form is expressed as $\overline{R} = \int_{-\infty}^{\infty} R(\omega)A(\omega)d\omega$.

The dependence of tropical CRE on ω (Fig. 1a) and the area PDF of ω (Fig. 1c) in a coupled climate model are analogous to the observed functions [cf. Fig. 2 in Bony et al. (2004)]. For ascending ($\omega < 0$) and weakly descending ($\omega > 0$) regions, the longwave and shortwave CREs vary approximately linearly with mid-tropospheric vertical velocity (Fig. 1a). For the longwave CRE, the positive (i.e., heating) values in strongly ascending regions such as the ITCZ reflect high-altitude cloud tops and large cloud fractions which together produce a strong greenhouse effect. The decreasing longwave CRE with increasing ω is due to cloud-top altitudes and cloud fractions reducing for weaker ascent regimes. For the shortwave CRE (Fig. 1a), the decreasing cooling effect as ascending motion weakens is likely due to a decreasing cloud fraction and consequently less shortwave reflection to space. The relative insensitivity of longwave and shortwave CRE to

changes in ω in strongly descending regions is likely a result of cloud-masking effects (Soden et al. 2004) and also suggests that the altitude and fraction of low clouds may not be strongly controlled by mid-tropospheric vertical velocity (Bony et al. 2004) but rather by other processes.

Although we would not necessarily expect the dependence of CSRE on vertical velocity to be as strong as the CRE dependence, it is plausible that regions of large-scale ascent would be moister than regions of descent, which would imprint on the CSRE. Indeed tropical ascending regions are observed to have reduced clear-sky outgoing longwave radiation relative to descending regions (Bony et al. 1997); this CSRE dependence on ω is at least qualitatively captured by climates models (Fig. 1b). There is also a simulated dependence of clear-sky shortwave radiation on vertical velocity (Fig. 1b), with regions of strong descent ($\omega > 30\,\mathrm{hPa}$) having a larger outgoing shortwave flux (presumably because the atmosphere in these descending regions is dry consequently absorbs less shortwave radiation). The area PDF of tropical ω in a climate model shows a skewed distribution in tropical regions (Fig. 1c), with a large area covered by slow-moving descending air [these are the so-called "radiator fins" where the longwave CRE is weak (Pierrehumbert 1995)]. The area PDF has a smaller ascent region with a larger variance in vertical velocity compared to the descent region. This area PDF from a climate model is qualitatively similar to an area PDF calculated using reanalysis data (Bony et al. 2004).

The dynamic component of changes in CRE for a given climate forcing is identified as the CRE change induced by the change in $A(\omega)$ [for fixed $R(\omega)$], which in general could be due to a change in the areas occupied by ascending vs descending air or re-organisations of the circulation within the ascending and descending regimes. It should be noted that dynamical processes, for example lower-tropospheric mixing, that might be decoupled from mid-tropospheric vertical velocity do not form part of our defined dynamic component and are instead included in the thermodynamic component (Wyant et al. 2006). The thermodynamic component represents the change in TOA

radiation for fixed $A(\omega)$, and includes effects such as a change in cloud optical depth or an increase in water-vapor concentration that accompany a warming atmosphere. The nonlinear component represents the combined effect of changes in thermodynamic and dynamic processes. We apply this decomposition not only to the CRE as in Bony et al. (2004), but also to the ASRE and the CSRE. The decomposition is expressed mathematically as:

$$\overline{\delta R} = \underbrace{\int_{-\infty}^{\infty} R(\omega)\delta A(\omega)d\omega}_{\text{dynamic}} + \underbrace{\int_{-\infty}^{\infty} \delta R(\omega)A(\omega)d\omega}_{\text{thermodynamic}} + \underbrace{\int_{-\infty}^{\infty} \delta R(\omega)\delta A(\omega)d\omega}_{\text{nonlinear}} \tag{1}$$

where $\overline{\delta R}$ is the change in either the total (shortwave + longwave) CRE, CSRE or ASRE averaged over all vertical velocities in the defined domain. We define the atmospheric dynamics feedback to be equal to $\overline{\delta R}$.

Our method of evaluating the decomposition (1) differs from that of Bony et al. (2004) in a number of respects. Firstly, we perform the decomposition globally, not only for tropical regions, and construct the $R(\omega)$ functions and the area PDFs using a vertically-averaged ω between 400 hPa and 500 hPa (our results are qualitatively similar when we average ω over the full atmosphere). Secondly, to understand how circulation changes at different latitudes influence the atmospheric dynamics feedback, we perform the decomposition at each latitude individually rather than over a large region. If CRE, CSRE and ASRE were solely functions of ω, then it would be possible to construct $R(\omega)$ using global data and then trace back to latitude to understand the influence of circulation changes in different regions on TOA radiation. However, these radiative effects depend not only on ω but also on temperature, latitude, relative humidity, and other factors. Consequently, constructing $R(\omega)$ functions using global data and then using these functions to determine dynamic

and thermodynamic feedbacks at a particular latitude is not possible as the local TOA radiation budget does not close. The ω limits of the $R(\omega)$ and $A(\omega)$ functions are specified to be the maximum and minimum values of the vertically-averaged vertical velocity at each latitude, and we use 21 equally-spaced ω 'bins'. If there are ω bins that are empty when constructing $R(\omega)$, we use a linearly interpolated form of $R(\omega)$ for which the missing value(s) are filled in when calculating the various terms in the decomposition (1). We now use this method to calculate the dynamic and thermodynamic contributions to changes in TOA radiation in coupled climate models.

3. Atmospheric dynamics feedback in coupled climate models

a. Simulations

We investigate the role of the large-scale atmospheric circulation in controlling TOA radiative anomalies using simulations from the Coupled Model Intercomparison Project Phase 5 (CMIP5) (Taylor et al. 2012). In particular, we analyze changes in TOA radiative fluxes for 27 models[2] between pre-industrial control runs (*piControl*) and runs in which the CO_2 concentration is instantaneously quadrupled relative to the pre-industrial level (*abrupt4xCO2*). The $R(\omega)$ and $A(\omega)$ functions for the *piControl* runs are constructed for each climatological month using 100 years of simulation data. These functions are then re-calculated for each month and year in the *abrupt4xCO2* runs to assess [using the decomposition (1)] how changes in dynamic and thermodynamic processes contribute to TOA radiative anomalies induced by the increase in CO_2. In our calculation of the atmospheric dynamics feedback, we exclude the first year following CO_2 quadrupling so as

[2]The models analyzed in this study are: ACCESS1-0, ACCESS1-3, BCC-CSM1-1, BCC-CSM1-1-M, CanESM2, CCSM4, CNRM-CM5, CNRM-CM5-2, CSIRO-Mk3-6-0, FGOALS-g2, FGOALS-s2, GFDL-CM3, GFDL-ESM2G, GFDL-ESM2M, GISS-E2-H, GISS-E2-R, HadGEM2-ES, INMCM4, IPSL-CM5A-LR, IPSL-CM5B-LR, MIROC5, MIROC-ESM, MPI-ESM-LR, MPI-ESM-MR, MPI-ESM-P, MRI-CGCM3, and NorESM1-M

to remove the effect of rapid circulation responses. It has been argued that it is more appropriate to think of these rapid adjustments, particularly of clouds, to an imposed TOA perturbation of being part of the climate forcing rather than the climate feedback (Zelinka et al. 2013). Later in this section we will compare the influences of rapid circulation adjustments vs slower, temperature-mediated adjustments on TOA radiative anomalies.

b. Atmospheric dynamics feedback vs latitude

The multimodel-mean changes in ASRE, CSRE, and CRE between the *abrupt4xCO2* and *piControl* simulations are plotted in Figure 2, along with the thermodynamic and dynamic + nonlinear components of these responses. Due to a strong compensation between the dynamic and nonlinear components, we show the sum of these components rather than each individually (a discussion of the factors controlling the magnitude of the nonlinear component is provided later in this section). For the remainder of the paper, we will refer to the sum of the dynamic and nonlinear terms as the dynamic term for simplicity.

1) ALL-SKY AND CLEAR-SKY RADIATIVE EFFECTS

For the ASRE (Fig. 2a) and CSRE (Fig. 2b), the total radiative anomalies are negative and warming (i.e., reduced net upward fluxes at TOA) at almost all latitudes following a quadrupling of CO_2.The thermodynamic component typically dominates the total radiative anomaly but the dynamic component is significant in the tropcis. For the clear-sky anomalies, changes in the large-scale circulation contribute on the order of $1\,\mathrm{W\,m^{-2}}$ to the TOA anomalies, with a shortwave warming effect in the deep tropics and a predominantly longwave cooling effect just off the equator (Fig. 2b). This latitudinal clear-sky warming/cooling structure reflects changes in mid-tropospheric vertical velocity (Fig. 3): A strengthening of ascending motion in the core of

the ITCZ indicates increased mass and moisture convergence in that region, which increases atmospheric water vapor leading to enhanced shortwave absorption and a warming anomaly on the equator (Fig. 2b). Similarly, the weakening of the ascending motion on the equatorward flanks of the climatological ITCZ (Fig. 3) causes reduced moisture convergence in those regions (at constant temperature) and decreases in water vapor and the longwave greenhouse effect. This pattern of tropical vertical velocity changes has been termed the "deep-tropics squeeze" (Lau and Kim 2015) and reflects a narrowing of the ITCZ under global warming (Byrne and Schneider 2016b). The reduced descent on the poleward sides of the ITCZ (Fig. 3) is also consistent with reduced atmospheric moisture divergence by the large-scale circulation (particularly in the Southern Hemisphere) leading to enhanced shortwave absorption, a negative radiative anomaly at TOA, and warming (Fig. 2b).

2) Cloud radiative effect

For the CRE (Fig. 2c), there is considerable latitudinal structure which reflects the complex and competing interactions between different cloud types and radiation in a changing climate (e.g., Ceppi et al. 2017). Within approximately 30° of the equator, the dynamic component of the change in CRE has roughly the same magnitude as the thermodynamic component, emphasizing the importance of large-scale atmospheric dynamics in controlling the spatial structures of tropical and subtropical cloud feedbacks. On the equatorward flanks of the ITCZ, where there is a downward acceleration of the large-scale circulation (weakened ascent) following CO_2 quadrupling (Fig. 3), we note a strongly warming shortwave cloud radiative anomaly (Fig. 2c). This likely reflects a decrease in shallow marine clouds with global warming (Bony and Dufresne 2005; Vial et al. 2013; Brient and Schneider 2016) and potentially a narrowing of the ITCZ, though other mechanisms are also likely to be involved. The dynamic shortwave contribution to the positive cloud feedback

in subtropical regions may be a result of a weakening of the subsidence in low-cloud regions and a consequent increase in cloud thickness and albedo (Ceppi et al. 2017). The positive (warming) dynamic shortwave cloud feedback in the tropics is cancelled to some extent by a negative (cooling) longwave feedback which is likely caused by the narrowing of the ITCZ with warming (Byrne and Schneider 2016b), which would reduce the longwave greenhouse effect of high clouds at the edges of the ITCZ. The positive cloud feedback in (particularly northern) mid-latitudes (Fig. 2c) is likely due to a poleward shift of the mid-latitude storm tracks towards latitudes with reduced shortwave insolation (Grise et al. 2013).

3) Fast vs slow dynamic responses

Cloud radiative feedbacks are typically divided into "cloud adjustments", which emerge rapidly in response to a radiative forcing, and surface temperature-mediated adjustments which evolve slowly as the climate warms (Kamae et al. 2015). The atmospheric dynamics feedback also has fast and slow components for the cloud and clear-sky feedbacks (Fig. 4). Poleward of approximately 30°, the dynamic components are similar in the first year ("fast") and averaged over years 91-100 ("slow") following the quadrupling of CO_2. Equatorward of 30°, however, there are considerable differences between the fast and slow dynamic responses. In the deep tropics, close to the equator, both the clear-sky and cloud responses are strongly positive (warming) 91-100 years after the quadrupling of CO_2 but are much smaller in the first year. This slow response is consistent with the ascent at the core of the ITCZ intensifying considerably between the two time periods analyzed (not shown).

The vertically-integrated atmospheric moist static energy (MSE) budget can be used diagnostically to understand the physical processes influencing tropical ω (Byrne and Schneider 2016a). Changes in the net energy input to the atmosphere (e.g., through TOA radiative anomalies) influ-

ence the MSE budget and consequently ω, and can be a fast response to CO_2 forcing. On the other hand, poleward transport of MSE by large-scale mean advection and transient eddies also affects tropical ω and depends fundamentally on meridional MSE gradients (Byrne and Schneider 2016a); these gradients would be expected to evolve slowly in response to CO_2 forcing as sea-surface temperatures increases. It is unclear why the dynamic components of the CRE and CSRE respond on different timescales at low and high latitudes – understanding these contrasting responses is a topic for future work. The different circulation-response timescales at different latitudes will be shown later to influence the global feedback parameter and the response of the Earth system to CO_2 forcing.

Finally, there is only a weak correlation between the globally-averaged fast and slow components of the dynamics feedback ($r = 0.38$). This weak relationship between the fast and slow components casts doubt on the feasibility of using the fast component to understand the long-term influence of changes in atmospheric circulation on TOA radiation [this is in contrast to the fast and slow responses of tropical precipitation changes, which have been shown to be strongly determined by the fast circulation response (Bony et al. 2013)].

4) "UP-DOWN" AND "MIX" COMPONENTS OF THE DYNAMICS FEEDBACK

In an influential paper on the energetics of tropical climate, Pierrehumbert (1995) used a simple two-box model to argue that "the warm pool sea surface temperature is very sensitive to [...] the relative area of the dry versus convective regions". Expressed in an equivalent way, Pierrehumbert (1995) was suggesting that the ratio of the areas of tropical ascent vs descent regions is an important controller of tropical climate. A widening of the Hadley circulation and a narrowing of the ITCZ are expected to occur as climate warms, resulting in a decrease in the area of tropical ascent relative to the tropical descent area (Byrne and Schneider 2016b). We have calculated the

total dynamics feedback but it is also of interest to isolate the portion of this feedback that is due to a change in the up-down area ratio (e.g., due to ITCZ narrowing) and the portion that is due to strengthening and weakening of the circulation within the ascent and descent regimes (e.g., due to a slowdown of the Walker circulation).

We decompose the total dynamics feedback into two parts: The first part corresponds to changes in the up-down area ratio (the "up-down component") and the second part corresponds to changes in the vertical velocity distribution within the separate "up" and "down" regimes (the "mix component"). The two components can be expressed mathematically as follows:

$$\begin{aligned} &\int_{-\infty}^{\infty} R(\omega)\delta A(\omega)d\omega = \\ &\underbrace{\int_{-\infty}^{0} [R]^{\mathrm{u}}[\delta A]^{\mathrm{u}}d\omega + \int_{0}^{\infty} [R]^{\mathrm{d}}[\delta A]^{\mathrm{d}}d\omega}_{\text{up-down component}} + \\ &\underbrace{\int_{-\infty}^{0} (R-[R]^{\mathrm{u}})(\delta A-[\delta A]^{\mathrm{u}})d\omega + \int_{0}^{\infty} (R-[R]^{\mathrm{d}})(\delta A-[\delta A]^{\mathrm{d}})d\omega}_{\text{mix component}} \end{aligned} \tag{2}$$

where $[\cdot]^{\mathrm{u}}$ indicates an average over all ascent regimes and $[\cdot]^{\mathrm{d}}$ is an average over all descent regimes.

Applying the decomposition (2) to the previously discussed dynamics feedback, we find that the up-down and mix components both contribute to the total dynamics feedback (Fig. 5). For the clear-sky anomalies, the up-down component is larger in the tropics (Fig. 5a), with relatively large cooling tendencies (of order $1\,\mathrm{W\,m^{-2}}$) on the equatorward flanks of the ITCZ. These cooling tendencies reflect atmospheric drying and reduced shortwave absorption and longwave greenhouse effect due to the narrowing of the ITCZ and the shift from ascending to descending motion in those regions. In the tropics, the mix component is a weak warming tendency and results from an acceleration of ascending motion in the core of the ITCZ and an associated enhancement of mois-

ture convergence. Interestingly, the mix component dominates the clear-sky dynamics feedback (Fig. 5b).

Overall, the influence of changes in the tropical up-down area ratio is weak compared to the influence of thermodynamic processes (cf. Fig. 2). This result contrasts with the findings of Pierrehumbert (1995) based on a simple two-box model of tropical climate, and casts doubt on the ability of changes in the widths of the ITCZ or Hadley circulation (in isolation) to strongly influence global climates of the past or the future.

5) Size of the nonlinear component

To gain insight into the size of the nonlinear component relative to the dynamic component, it is instructive to assume R is approximately a linear function of ω, i.e., $R(\omega) = a + b\omega$. The assumption of linearity is reasonable in climate models over the majority of tropical ω regimes for both CRE (Fig. 1a) and CSRE (Fig. 1b). Taking the definitions of the dynamic and nonlinear components (1), substituting $R(\omega) = a + b\omega$ and rearranging, the ratio of the nonlinear component to the dynamics component can be shown to be equal to $\delta b/b$, where δb is the change in the slope of $R(\omega)$ between the *piControl* and *abrupt4xCO2* runs. For CRE, $\delta b/b \approx -20\%$ meaning that the sensitivity of CRE to changes in mid-tropospheric vertical decreases by 20% under global warming (in climate models). This weakening of the relationship between vertical velocity and CRE as the climate warms could be a result of cloud-masking effects associated with rising CO_2 and water-vapor concentrations in the atmosphere. This simple analysis suggests that the nonlinear component of CRE changes is approximately 20% of the magnitude of the dynamic component, and of the opposite sign. This estimated magnitude of the nonlinear component roughly matches the values calculated explicitly using the decomposition (1) in the tropics (not shown). However, at higher latitudes the nonlinear component is a larger fraction of the dynamic component. This

enhanced importance of nonlinear effects outside the tropics is potentially due to the assumption of linear $R(\omega)$ being less valid at these latitudes, and/or the magnitude of the fractional change in the slope of $R(\omega)$ with warming (i.e., $\delta b/b$) being larger because of stronger masking effects.

c. Global atmospheric dynamics feedback

Averaged over all latitudes, TOA radiative anomalies induced by CO_2 quadrupling are almost entirely a result of thermodynamic processes (Fig. 6). Although the atmospheric dynamics feedback is relatively important at low latitudes (Fig. 2), there is an almost complete cancellation of positive and negative feedbacks when the global average is calculated. Below we explain why the atmospheric dynamics feedback is small when averaged over large regions.

1) MASS BUDGET CONSTRAINT

That the global atmospheric dynamics feedback is close to zero is perhaps not surprising when the constraint of the atmospheric mass budget is taken into account. Within a region that has a negligible mean mass flux across its boundaries [the region occupied by the Hadley circulation, for example, provided transient-eddy mass fluxes are small], the steady-state mass budget can be expressed as:

$$\int_{-\infty}^{0} \omega A(\omega) d\omega = -\int_{0}^{\infty} \omega A(\omega) d\omega. \tag{3}$$

This expression stipulates that in the atmosphere, the area of upward motion multiplied by the average upward velocity is equal to the area of downward motion multiplied by the average downward velocity. We now illustrate how the mass budget places a strong constraint on the ability of changes in the atmospheric circulation to influence TOA radiation or global climate change.

As in our discussion of the nonlinear component above, a useful starting point is to assume the dependence of TOA radiation on mid-tropospheric vertical velocity is linear, i.e. $R(\omega) = a + b\omega$. Linearity is not an unreasonable assumption for climate models, at least for tropical ω regimes with a heavy area weighting (Fig. 1). The linearity assumption is also supported by satellite observations of CRE (Wyant et al. 2006). Using this assumption, the dynamic component of changes in TOA radiation is given by: $\int_{-\infty}^{\infty} R(\omega)\delta A(\omega)d\omega = a\int_{-\infty}^{\infty}\delta A(\omega)d\omega + b\int_{-\infty}^{\infty}\omega\delta A(\omega)d\omega$. By construction of the area PDFs, $\int_{-\infty}^{\infty}\delta A(\omega)d\omega = 0$, and from the atmospheric mass budget (3) it follows that $\int_{-\infty}^{\infty}\omega\delta A(\omega)d\omega = 0$. Consequently, for a linear relationship between TOA radiation and large-scale vertical velocity, the impact of changes in atmospheric circulation averaged over a closed-mass region is expected to be zero. A slightly modified argument can be used to show that the nonlinear component is also zero for linear $R(\omega)$. The implications of a linear $R(\omega)$ for the dynamic component of TOA radiative anomalies have also been discussed by Wyant et al. (2006).

2) Effect on global climate change

Although small in magnitude, the globally-averaged atmospheric dynamics feedback nevertheless has an influence on the climate response to CO_2 quadrupling (Figs. 6 and 7). For the Equilibrium Climate Response (ECR), defined here as the equilibrium change in near-surface temperature following CO_2 quadrupling calculated using the regression method of Gregory et al. (2004), the dynamics feedback marginally increases the surface warming (Figs. 6 and 7a); the multimodel-mean ECR is 0.2 K larger than that predicted by the thermodynamic component alone. There is a weak correlation ($r = -0.51$) between the all-sky dynamics feedback (globally averaged) and ECR, indicating that differences in atmospheric circulation responses across models [or in climatological $R(\omega)$ relationships across models, see (1)] explain approximately 25% of the intermodel spread in ECR.

The global feedback parameter, or the slope of the linear regression of TOA all-sky radiative anomalies vs near-surface temperature anomalies (excluding the rapid adjustments in year 1 of the imposed forcing), describes the efficiency with which the Earth system balances a radiative forcing. The feedback parameter is the average of all the individual feedbacks (i.e., water-vapor, cloud, lapse-rate feedbacks) and is typically positive, meaning that the net outward flux of radiation at TOA increases as the surface temperature increases during equilibration. The atmospheric dynamics feedback robustly makes the global feedback parameter less positive (Figs. 6 and 7b) implying that the Earth system is less efficient at eliminating a TOA perturbation because of circulation changes. This reduction in the feedback parameter is consistent with the all-sky TOA cooling radiative anomaly associated with circulation changes becoming smaller over time following the quadrupling of CO_2 (Figs. 4a and 6). Expressed a different way, the global response of the atmospheric circulation is a small and positive feedback on climate change (the opposite of an iris effect) and tends to increase the surface temperature response to a given TOA radiative forcing. This globally-averaged dynamics feedback masks considerable latitudinal structure as we discussed previously (see Fig. 2a).

The atmospheric circulation response to climate change increases the global feedback parameter, requiring a larger ECR to balance a given TOA forcing. However, the circulation response makes the adjusted radiative forcing less negative (Fig. 7c) which tends to reduce the ECR. Averaged over all models, the fast adjustment of the atmospheric circulation gives a TOA cooling of $0.23\,\mathrm{W\,m^{-2}}$ which is strongly correlated with the dynamical cloud adjustment (for each model this fast dynamical adjustment is estimated as the y-intercept of a linear fit of the red points in Figure 6). The physical mechanisms controlling the rapid response of the atmospheric circulation and concurrent TOA cooling require further investigation. The competing influences of circulation

changes on ECR, via the effects on the feedback parameter and adjusted radiative forcing, result in only a weak influence of dynamics on ECR (Fig. 7a).

The climate models examined here are unable to simulate various processes, such as convective aggregation, that have been put forward as potentially important influencers of global climate (Bony et al. 2016). Furthermore, climate models struggle to accurately simulate clouds (Pincus et al. 2008), and it is plausible that important nonlinearities in the $R(\omega)$ relationship, not captured by climate models, could lead to TOA radiative anomalies that are substantially non-zero on global scales. In the next section we will use an idealized GCM with prescribed TOA forcings to investigate how hypothetical atmospheric dynamics feedbacks, potentially induced by the effects mentioned above but not simulated by the current generation of climate models, could influence global climate.

4. Effectiveness of high- vs low-latitude dynamics feedbacks

a. Idealized forcing simulations

We use a moist idealized GCM perturbed by stylized TOA forcing profiles to investigate in a general way how the latitudinal structure of the atmospheric dynamics feedback could impact global climate. Simulations are performed using the slab-ocean aquaplanet GCM of O'Gorman and Schneider (2008), which is based upon the model of Frierson et al. (2006) and Frierson (2007). The GCM is run at a horizontal spectral resolution of T42 with 10 vertical levels and the surface heat capacity is equivalent to 1m of liquid water. The model uses a simplified two-stream gray radiation scheme with a prescribed longwave optical thickness; shortwave fluxes are specified as a function of latitude and longitude [see O'Gorman and Schneider (2008) for full details of the

radiation scheme]. It is important to note that this model does not simulate water vapor or cloud feedbacks.

We perform a control simulation (without prescribed TOA forcing) with a climate that is roughly similar to that of the present-day Earth along with three perturbed simulations with prescribed TOA longwave forcings (Fig. 8a): A tropical forcing from $\phi = -30^\circ$ to 30° and an extratropical forcing ($\phi = -90^\circ$ to -30° and $\phi = 30^\circ$ to 90°), both with a global-mean forcing of $4\,\mathrm{W\,m^{-2}}$, and a global-wave forcing with a maximum amplitude of $4\,\mathrm{W\,m^{-2}}$ and a global mean of $0\,\mathrm{W\,m^{-2}}$. Each simulation is spun up for 1000 days with averages taken over the subsequent 2000 days. The magnitudes of the stylized forcings are considerably larger than what we have calculated for the atmospheric dynamics feedback in the fully-coupled simulations (cf. Fig. 2), and the latitudinal structures imposed here are also highly idealized. However, our objective is to understand the effectiveness of low-latitude vs high-latitude forcings (due to changes in atmospheric circulation or other processes) in changing global climate, and for this purpose using an idealized GCM and stylized forcings is an appropriate first step.

b. Surface temperature responses

Although the tropical and extratropical forcings have equal magnitudes in the global mean, they induce strikingly different surface temperature responses (Fig. 8b). The temperature response to extratropical forcing (1 K) is greater than twice the magnitude of the response to tropical forcing (0.4 K). This stronger sensitivity of global climate to extratropical vs tropical forcing has also been discovered for surface forcings (Rose et al. 2014; Rugenstein et al. 2016) – ocean heat uptake at high latitudes cools the climate more efficiently than the same heat uptake at low latitudes. Indeed, the difference in efficiency between low- and high-latitude forcings (a factor of approximately 2) is comparable for our TOA forcing simulations and for simulations forced by ocean heat uptake

patterns (Rose et al. 2014). To further emphasize how the latitudinal pattern of TOA forcing influences the global temperature, the global-wave forcing has a global-mean magnitude of zero (Fig. 8a) and yet induces a surface temperature cooling of 0.2 K.

The physical mechanisms leading to the enhanced climate response to high-latitude vs low-latitude forcings has received considerable attention (e.g., Langen and Alexeev 2007; Pithan and Mauritsen 2014; Rose et al. 2014; Roe et al. 2015). Fundamentally, the contrasting temperature responses are driven by different sensitivities of poleward atmospheric energy transport to high-latitude and low-latitude temperature perturbations as well as latitudinal variations in local radiative feedbacks [see Rose et al. (2014) for an insightful discussion on this topic]. Consequently, although the simplified GCM used here omits a variety of processes which might be expected to change the magnitude of the climate response to TOA forcings (e.g., water-vapor and ice-albedo feedbacks), we believe the larger climate sensitivity to high-latitude forcing is a robust result as it is grounded in well-established physical mechanisms.

The idealized simulations discussed in this section have important implications for the atmospheric dynamics feedback. Although the influence of circulation changes on the Earth's global radiative balance is constrained to be weak (as discussed above), the effect of circulation changes on TOA radiative anomalies at different latitudes is non-negligible, and the global temperature response to circulation changes is likely to depend on this latitudinal structure. Furthermore, discussions of how the atmospheric circulation response might mitigate climate change have focused largely on tropical iris-type mechanisms (e.g., Pierrehumbert 1995; Lindzen et al. 2001; Mauritsen and Stevens 2015; Bony et al. 2016). Based on the idealized simulations presented here, a $10\,\mathrm{W\,m^{-2}}$ tropical TOA forcing would be needed to change global surface temperature by 1 K. Our analysis of the atmospheric dynamics feedback in global climate models suggests a circulation-induced tropical TOA radiative anomaly of no greater than 1-2 $\mathrm{W\,m^{-2}}$ under CO_2

quadrupling. Furthermore, an observational analysis shows that convective aggregation also has a weak influence on net TOA radiation [of order $1\,\mathrm{W\,m^{-2}}$ (Tobin et al. 2012)]. Consequently, we argue that the relative insensitivity of global climate to tropical TOA perturbations, combined with these area-averaged perturbations due to changes in the atmospheric circulation being constrained to be small, means that tropical iris-type mechanisms are unlikely to exert a substantial influence on past or future climate change.

5. Summary and discussion

The response of the atmospheric circulation to radiative forcing, via its influence on clouds and water vapor, has been put forward as a potentially important feedback on climate change (e.g., Lindzen et al. 2001). Here, using a method based on that of Bony et al. (2004), we have calculated for the first time the atmospheric dynamics feedback at each latitude in a range of climate models subjected to an abrupt CO_2 quadrupling. For all-sky and clear-sky TOA radiative anomalies, the dynamics feedback is generally smaller than the thermodynamics feedback, though is not entirely negligible, particularly in the tropics where its magnitude peaks at roughly $1\,\mathrm{W\,m^{-2}}$. For changes in CRE, the dynamics feedback is comparable to the thermodynamics feedback within approximately 30° of the equator. The latitudinal pattern of the dynamic component of CRE changes reflects previously identified changes in the tropical circulation including enhanced ascent in the core of the ITCZ, a narrowing of the ITCZ, and weaker descent in subtropical regions. This coupling between CRE and circulation emphasizes the necessity of understanding the sensitivity of large-scale atmospheric dynamics to climate change in order to fully understand the cloud feedback.

At individual latitudes, the atmospheric dynamics feedback is comparable to the thermodynamics feedback. However, a large degree of cancellation between positive and negative dynamics

feedbacks at different latitudes results in the thermodynamic component dominating the global TOA response. That the global-mean atmospheric dynamics feedback is close to zero is shown to be a consequence of (i) the steady-state atmospheric mass budget and (ii) approximately linear relationships between mid-tropospheric vertical velocity and CRE and CSRE. This fundamental constraint raises doubts regarding the feasibility of iris-type mechanisms (e.g., convective aggregation) for mitigating climate change.

Although the global TOA radiative anomalies induced by circulation changes are small relative to anomalies induced by thermodynamic processes (e.g., temperature-driven changes in water vapor), they do affect the global response to CO_2 quadrupling. In particular, circulation changes decrease the global feedback parameter, leading to the Earth system becoming less efficient at balancing a given radiative forcing which, all else equal, would result in a larger climate sensitivity. This warming influence of circulation changes is counteracted to some degree by the effect on the adjusted radiative forcing, which is reduced by circulation changes. These competing influences of dynamics on the climate response result in a multimodel-mean increase in ECR of 0.2 K (or approximately 3% of the total warming) – circulation changes tend to modestly enhance the global warming resulting from CO_2 increases. Despite this minor influence on ECR, the dynamic component is weakly correlated with the ECR spread across models, opening up the possibility of using the atmospheric dynamics feedback as a new constraint on climate sensitivity.

We performed idealized-GCM simulations to assess how hypothetical circulation-induced TOA anomalies at low and high latitudes, due to unresolved dynamical processes such as convective aggregation, could affect global climate. We showed that a high-latitude forcing is twice as effective as a low-latitude forcing in changing global surface temperature (interestingly, we also found that a hemispherically symmetric forcing, with a global mean of zero, can induce a non-zero global temperature response). These results further strengthen our argument that low-latitude dynamical

responses to climate change – such as convective aggregation or ITCZ narrowing – are unlikely to greatly influence global climate unless they are capable of inducing a very large TOA anomaly. On the other hand, circulation changes that create TOA anomalies at higher latitudes (such as a shift in the mid-latitude storm track) are expected to be twice as efficient at changing global surface temperature and are consequently should be a priority to understand and quantify.

Our findings suggest a number of avenues for future research. Decades of satellite measurements now enable observational estimates of the atmospheric dynamics feedback, using both decadal trends and differences between positive and negative phases of El Niño; such estimates would be a useful benchmark which with to assess our climate model results. These observations could also be examined in detail to assess whether nonlinearities in observed $R(\omega)$ relationships are sufficiently strong to generate atmospheric dynamics feedbacks that could meaningfully influence global climate. Our focus has been the influence of atmospheric circulation changes on TOA radiation and global temperature. However, the global precipitation response to climate change is linked to TOA as well as surface radiative anomalies (e.g., O'Gorman et al. 2012) – an interesting topic for future work would be to understand the contribution of circulation changes to the atmospheric (rather than the TOA) radiative budget and consequently to the response of global precipitation to climate change.

Acknowledgments. We thank Paulo Ceppi, Reto Knutti, Paul O'Gorman, and Maria Rugenstein for helpful discussions.

References

Allan, R. P., 2011: Combining satellite data and models to estimate cloud radiative effect at the surface and in the atmosphere. *Meteorological Applications*, **18**, 324–333.

Bony, S., G. Bellon, D. Klocke, S. Sherwood, S. Fermepin, and S. Denvil, 2013: Robust direct effect of carbon dioxide on tropical circulation and regional precipitation. *Nat. Geosci.*, **6**, 447–451.

Bony, S., and J. L. Dufresne, 2005: Marine boundary layer clouds at the heart of tropical cloud feedback uncertainties in climate models. *Geophys. Res. Lett.*, **32**, l20806.

Bony, S., J.-L. Dufresne, H. Le Treut, J.-J. Morcrette, and C. Senior, 2004: On dynamic and thermodynamic components of cloud changes. *Climate Dyn.*, **22**, 71–86.

Bony, S., K. M. Lau, and Y. C. Sud, 1997: Sea surface temperature and large-scale circulation influences on tropical greenhouse effect and cloud radiative forcing. *J. Climate*, **10**, 2055–2077.

Bony, S., B. Stevens, D. Coppin, T. Becker, K. A. Reed, A. Voigt, and B. Medeiros, 2016: Thermodynamic control of anvil cloud amount. *Proc. Natl. Acad. Sci.*, **113**, 8927–8932,.

Brient, F., and T. Schneider, 2016: Constraints on climate sensitivity from space-based measurements of low-cloud reflection. *J. Climate*, **29**, 5821–5835.

Byrne, M. P., and P. A. O'Gorman, 2015: The response of precipitation minus evapotranspiration to climate warming: Why the "wet-get-wetter, dry-get-drier" scaling does not hold over land. *J. Climate*, **28**, 8078–8092.

Byrne, M. P., and T. Schneider, 2016a: Energetic constraints on the width of the intertropical convergence zone. *J. Climate*, **29**, 4709–4721.

Byrne, M. P., and T. Schneider, 2016b: Narrowing of the ITCZ in a warming climate: Physical mechanisms. *Geophys. Res. Lett.*, **43**.

Ceppi, P., F. Brient, M. D. Zelinka, and D. L. Hartmann, 2017: Cloud feedback mechanisms and their representation in global climate models. *WIREs Climate Change*, doi:10.1002/wcc.465.

Chang, E. K. M., Y. Guo, and X. Xia, 2012: CMIP5 multimodel ensemble projection of storm track change under global warming. *J. Geophys. Res.: Atmos.*, **117 (D23)**.

Frierson, D. M. W., 2007: The dynamics of idealized convection schemes and their effect on the zonally averaged tropical circulation. *J. Atmos. Sci.*, **64**, 1959–1976.

Frierson, D. M. W., I. M. Held, and P. Zurita-Gotor, 2006: A gray-radiation aquaplanet moist GCM. Part I: Static stability and eddy scale. *J. Atmos. Sci.*, **63**, 2548–2566.

Fu, Q., M. Baker, and D. L. Hartmann, 2002: Tropical cirrus and water vapor: an effective Earth infrared iris feedback? *Atmos. Chem. Phys.*, **2**, 31–37.

Gregory, J. M., and Coauthors, 2004: A new method for diagnosing radiative forcing and climate sensitivity. *Geophys. Res. Lett.*, **31**.

Grise, K. M., L. M. Polvani, G. Tselioudis, Y. Wu, and M. D. Zelinka, 2013: The ozone hole indirect effect: Cloud-radiative anomalies accompanying the poleward shift of the eddy-driven jet in the Southern Hemisphere. *Geophys. Res. Lett.*, **40**, 3688–3692.

Kamae, Y., M. Watanabe, T. Ogura, M. Yoshimori, and H. Shiogama, 2015: Rapid adjustments of cloud and hydrological cycle to increasing CO_2: a review. *Curr. Clim. Change Rep.*, **1**, 103–113.

Kay, J. E., B. Medeiros, Y.-T. Hwang, A. Gettelman, J. Perket, and M. G. Flanner, 2014: Processes controlling Southern Ocean shortwave climate feedbacks in CESM. *Geophys. Res. Lett.*, **41**, 616–622.

Langen, P. L., and V. A. Alexeev, 2007: Polar amplification as a preferred response in an idealized aquaplanet GCM. *Climate Dyn.*, **29**, 305–317.

Lau, W. K. M., and K. M. Kim, 2015: Robust hadley circulation changes and increasing global dryness due to CO_2 warming from CMIP5 model projections. *Proc. Natl. Acad. Sci.*, **112**, 3630–3635.

Lindzen, R. S., M.-D. Chou, and A. Y. Hou, 2001: Does the Earth have an adaptive infrared iris? *Bull. Amer. Meteor. Soc.*, **82**, 417–432.

Lu, J., G. A. Vecchi, and T. Reichler, 2007: Expansion of the Hadley cell under global warming. *Geophys. Res. Lett.*, **34**, L06805.

Mauritsen, T., and B. Stevens, 2015: Missing iris effect as a possible cause of muted hydrological change and high climate sensitivity in models. *Nat. Geosci.*, **8**, 346–351.

Mbengue, C., and T. Schneider, 2017: Storm-track shifts under climate change: Toward a mechanistic understanding using baroclinic mean available potential energy. *J. Atmos. Sci.*, **74**, 93–110.

O'Gorman, P. A., 2010: Understanding the varied response of the extratropical storm tracks to climate change. *Proc. Natl. Acad. Sci.*, **107**, 19 176–19 180.

O'Gorman, P. A., R. P. Allan, M. P. Byrne, and M. Previdi, 2012: Energetic constraints on precipitation under climate change. *Surv. Geophys.*, **33**, 585–608.

O'Gorman, P. A., and T. Schneider, 2008: The hydrological cycle over a wide range of climates simulated with an idealized GCM. *J. Climate*, **21**, 5797–5806.

Pierrehumbert, R. T., 1995: Thermostats, radiator fins, and the local runaway greenhouse. *J. Atmos. Sci.*, **52**, 1784–1806.

573 Pincus, R., C. P. Batstone, R. J. P. Hofmann, K. E. Taylor, and P. J. Glecker, 2008: Evaluating the
574 present-day simulation of clouds, precipitation, and radiation in climate models. *J. Geophys.*
575 *Res.: Atmos.*, **113 (D14)**.

576 Pithan, F., and T. Mauritsen, 2014: Arctic amplification dominated by temperature feedbacks in
577 contemporary climate models. *Nat. Geosci.*, **7**, 181–184.

578 Ramanathan, V. L. R. D., R. D. Cess, E. F. Harrison, P. Minnis, B. R. Barkstrom, E. Ahmad,
579 D. Hartmann, and Coauthors, 1989: Cloud-radiative forcing and climate: Results from the
580 Earth Radiation Budget Experiment. *Science*, **243**, 57–63.

581 Roe, G. H., N. Feldl, K. C. Armour, Y.-T. Hwang, and D. M. W. Frierson, 2015: The remote
582 impacts of climate feedbacks on regional climate predictability. *Nat. Geosci.*, **8**, 135–139.

583 Rose, B. E. J., K. C. Armour, D. S. Battisti, N. Feldl, and D. D. B. Koll, 2014: The dependence of
584 transient climate sensitivity and radiative feedbacks on the spatial pattern of ocean heat uptake.
585 *Geophys. Res. Lett.*, **41**, 1071–1078.

586 Rugenstein, M. A. A., K. Caldeira, and R. Knutti, 2016: Dependence of global radiative feedbacks
587 on evolving patterns of surface heat fluxes. *Geophys. Res. Lett.*, **43**, 9877–9885.

588 Scheff, J., and D. Frierson, 2012: Twenty-first-century multimodel subtropical precipitation de-
589 clines are mostly midlatitude shifts. *J. Climate*, **25**, 4330–4347.

590 Seager, R., N. Naik, and G. A. Vecchi, 2010: Thermodynamic and dynamic mechanisms for
591 large-scale changes in the hydrological cycle in response to global warming. *J. Climate*, **23**,
592 4651–4668.

593 Shaw, T. A., and Coauthors, 2016: Storm track processes and the opposing influences of climate
594 change. *Nat. Geosci.*, **9**, 656–664.

595 Shepherd, T. G., 2014: Atmospheric circulation as a source of uncertainty in climate change
596 projections. *Nat. Geosci.*, **7**, 703.

597 Soden, B. J., A. J. Broccoli, and R. S. Hemler, 2004: On the use of cloud forcing to estimate cloud
598 feedback. *J. Climate*, **17**, 3661–3665.

599 Taylor, K. E., R. J. Stouffer, and G. A. Meehl, 2012: An overview of CMIP5 and the experiment
600 design. *Bull. Amer. Meteor. Soc.*, **93**, 485–498.

601 Tobin, I., S. Bony, and R. Roca, 2012: Observational evidence for relationships between the degree
602 of aggregation of deep convection, water vapor, surface fluxes, and radiation. *J. Climate*, **25**,
603 6885–6904.

604 Vecchi, G. A., and B. J. Soden, 2007: Global warming and the weakening of the tropical circula-
605 tion. *J. Climate*, **20**, 4316–4340.

606 Vial, J., J.-L. Dufresne, and S. Bony, 2013: On the interpretation of inter-model spread in CMIP5
607 climate sensitivity estimates. *Climate Dyn.*, **41**, 3339–3362.

608 Wall, C. J., and D. L. Hartmann, 2015: On the influence of poleward jet shift on shortwave cloud
609 feedback in global climate models. *J. Adv. Model. Earth Syst.*, **7**, 2044–2059.

610 Wing, A. A., K. Emanuel, C. E. Holloway, and C. Muller, 2017: Convective self-aggregation in
611 numerical simulations: A review. *Surv. Geophys.*, 1–25, doi:10.1007/s10712-017-9408-4.

612 Wing, A. A., and K. A. Emanuel, 2014: Physical mechanisms controlling self-aggregation of
613 convection in idealized numerical modeling simulations. *J. Adv. Model. Earth Syst*, **6**, 59–74.

614 Wodzicki, K. R., and A. D. Rapp, 2016: Long-term characterization of the Pacific ITCZ using
615 TRMM, GPCP, and ERA-Interim. *J. Geophys. Res.: Atmos.*, **121**, 3153–3170.

Wyant, M. C., C. S. Bretherton, J. T. Bacmeister, J. T. Kiehl, I. M. Held, M. Zhao, S. A. Klein, and B. J. Soden, 2006: A comparison of low-latitude cloud properties and their response to climate change in three AGCMs sorted into regimes using mid-tropospheric vertical velocity. *Climate Dyn.*, **27**, 261–279.

Yin, J. H., 2005: A consistent poleward shift of the storm tracks in simulations of 21st century climate. *Geophys. Res. Lett.*, **32 (18)**.

Zelinka, M. D., S. A. Klein, K. E. Taylor, T. Andrews, M. J. Webb, J. M. Gregory, and P. M. Forster, 2013: Contributions of different cloud types to feedbacks and rapid adjustments in CMIP5. *J. Climate*, **26**, 5007–5027.

LIST OF FIGURES

671 x-axes show the quantities calculated using only the thermodynamic component of the total
672 radiative anomalies. Hence, any departures from the one-to-one lines are due to changes in
673 the large-scale atmospheric circulation. 39

674 **Fig. 8.** (a) Imposed longwave TOA forcings (positive means heating) as a function of latitude for
675 three idealized simulations perturbed from the control run, and (b) the surface temperature
676 response for each perturbed simulation relative to the control run. The black lines correspond
677 to the tropical forcing, the red lines to the extratropical forcing, and the blue lines to the
678 global-wave forcing. Each forcing has a $\cos 3\phi$ functional form. 40

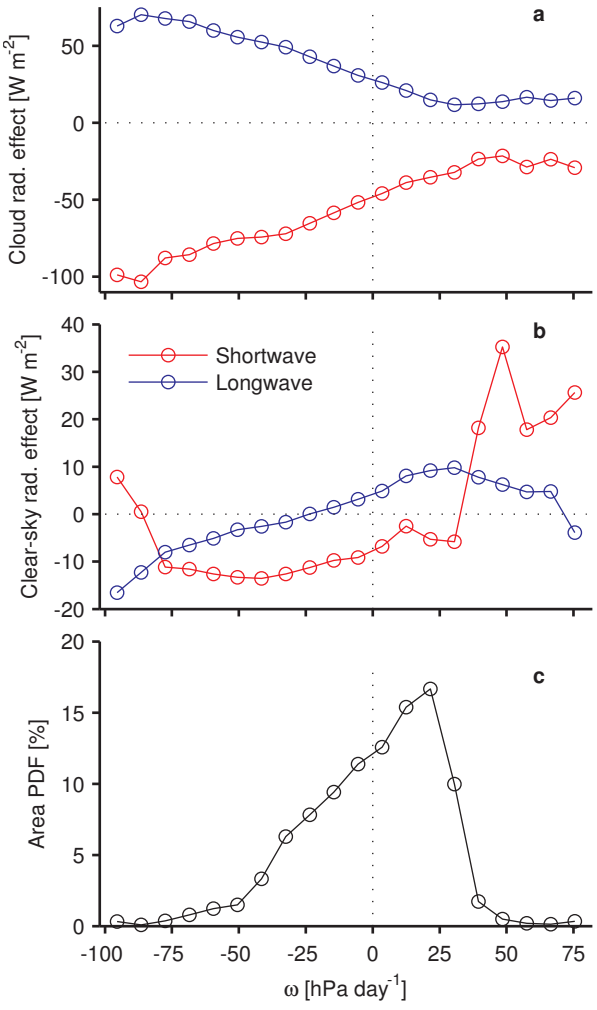

679 FIG. 1. The annual-mean tropical ($\phi = -30^\circ$ to 30°, where ϕ is the latitude) (a) cloud radiative effect, (b)
680 clear-sky radiative effect, and (c) area PDF of vertical velocity for a single climate model (MRI-CGCM3). For
681 the radiative effects, blue and red lines indicate the longwave and shortwave components, respectively. Each
682 dot represents a different ω bin (21 in total). The functions are constructed for each climatological month using
683 vertical velocities and radiative fluxes averaged over 100 years of the *piControl* simulation before the annual
684 means are taken. The longwave and shortwave components of the clear-sky radiative effect have had their
685 averages over all vertical velocity bins removed so as to emphasize the functional dependence on ω.

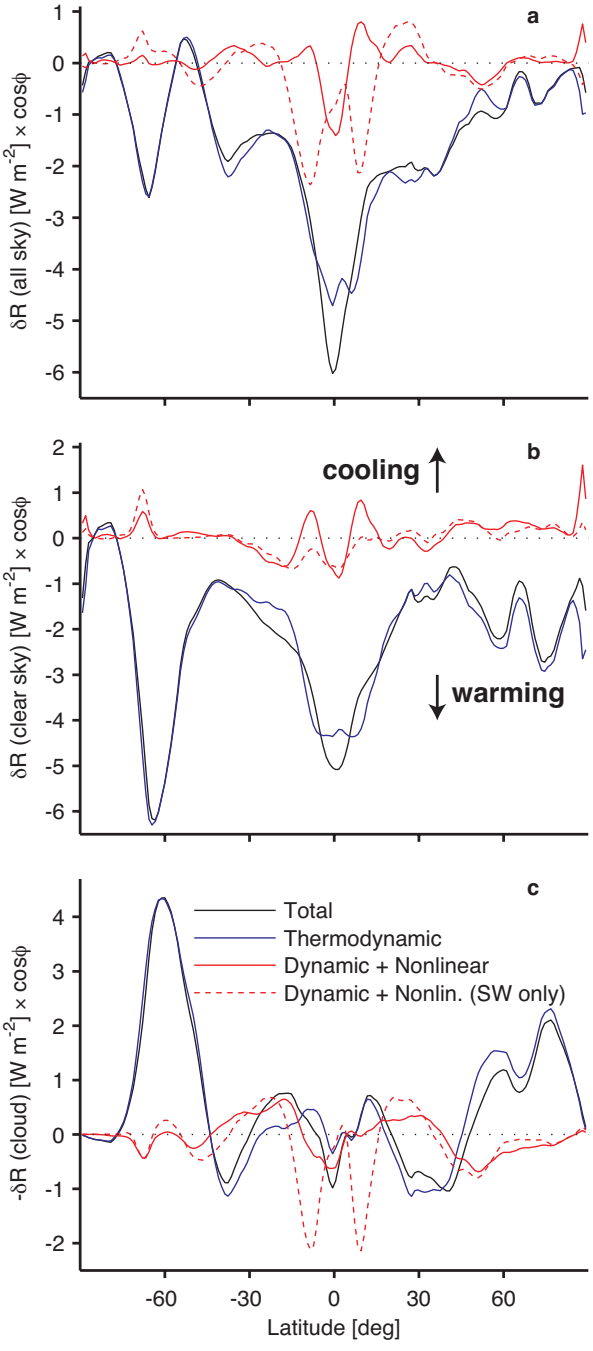

FIG. 2. Multimodel-mean changes in (a) all-sky radiative effect, (b) clear-sky radiative effect, and (c) cloud radiative effect vs latitude (black solid lines) between the *piControl* and *abrupt4xCO2* simulations. Each component has been averaged over years 2-100 of the *abrupt4xCO2* simulations. The thermodynamic (blue solid lines) and the dynamic + nonlinear components (red solid lines) for each forcing are also plotted, along with the shortwave contributions to the dynamic + nonlinear components (red dashed lines). Each term has been multiplied by a factor of $\cos\phi$ to reflect the decreasing area per degree latitude towards the poles. Note that minus the change in cloud radiative effect has been plotted so that negative and positive values correspond to warming and cooling, respectively, as for the all-sky and clear-sky panels.

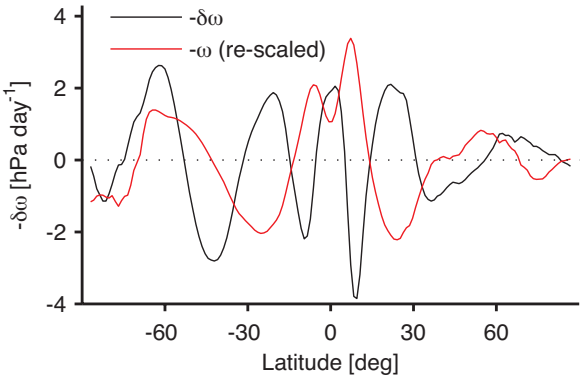

FIG. 3. Multimodel-mean change in (minus) the mid-tropospheric vertical velocity (averaged from 400hPa to 500hPa) between *piControl* and *abrupt4xCO2* (black line) along with (minus) the multimodel-mean vertical velocity from *piControl* (red line), which has been re-scaled by a factor of 0.15. For the change in vertical velocity, we average the *abrupt4xCO2* data over years 2-100 so as to remove the rapid circulation adjustments and be consistent with our calculation of the atmospheric dynamics feedback.

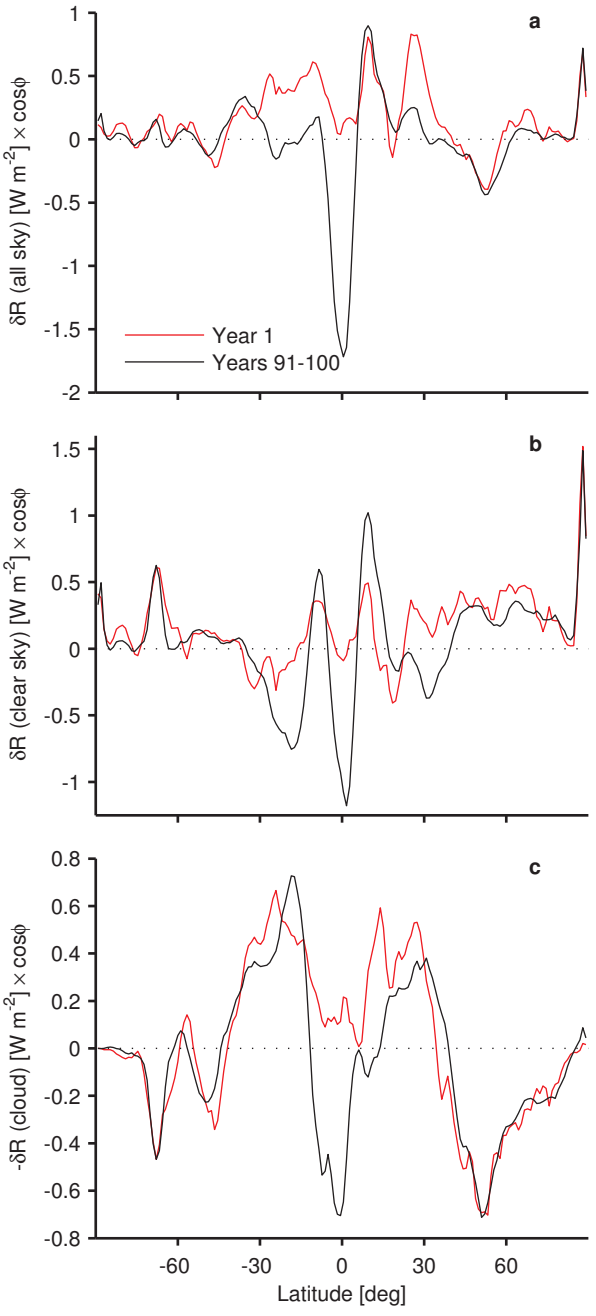

699 FIG. 4. Multimodel-mean dynamic + nonlinear components of the changes in (a) all-sky, (b) clear-sky,
700 and (c) cloud radiative effects between *piControl* and year 1 (red lines) and years 91-100 (black lines) of the
701 *abrupt4xCO2* simulations.

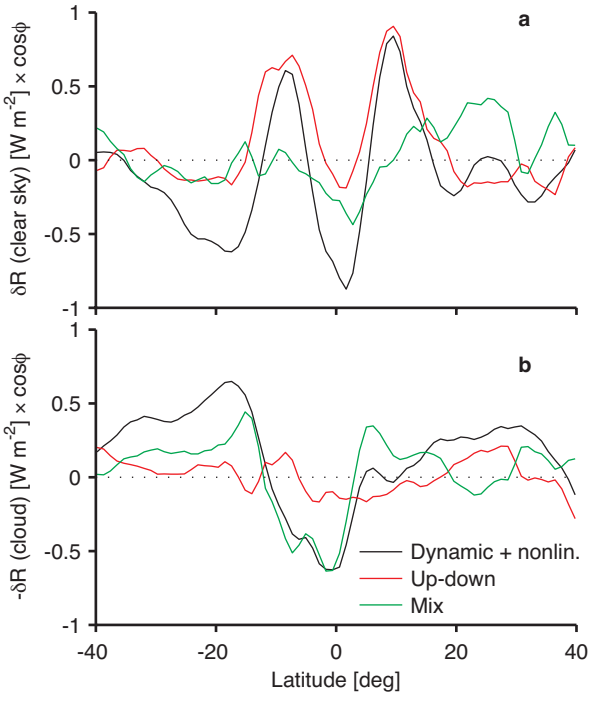

FIG. 5. Multimodel-mean dynamic + nonlinear components of the changes in (a) clear-sky and (b) cloud radiative effects between the *piControl* and *abrupt4xCO2* simulations (black lines). As discussed in section 3, year 1 of the *abrupt4xCO2* simulations is excluded so as to remove the effects of rapid circulation adjustments. The "up-down" (red lines) and "mix" contributions (green lines) to these components, as defined by (2), are also shown.

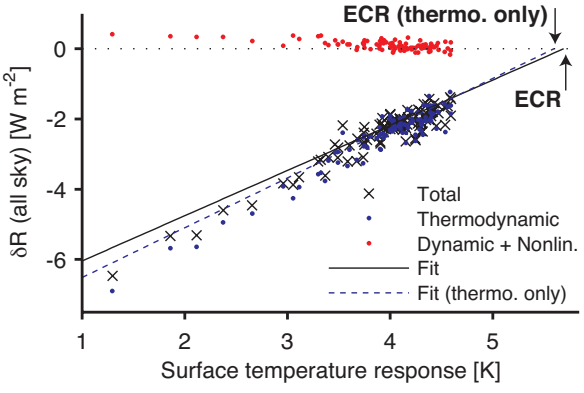

FIG. 6. Global top-of-atmosphere all-sky total radiative anomalies for the CCSM4 model (black crosses) as a function of near-surface temperature changes for the first 100 years following abrupt CO_2 quadrupling. The thermodynamic (blue dots) and dynamic + nonlinear components (red dots) are also shown, along with linear least-squares fits to the total top-of-atmosphere anomalies (black solid line) and the thermodynamic component of the anomalies (blue dashed line). The radiative anomalies in year 1 following CO_2 quadrupling are excluded from the linear fits. The estimated ECRs based on the linear fits are also indicated.

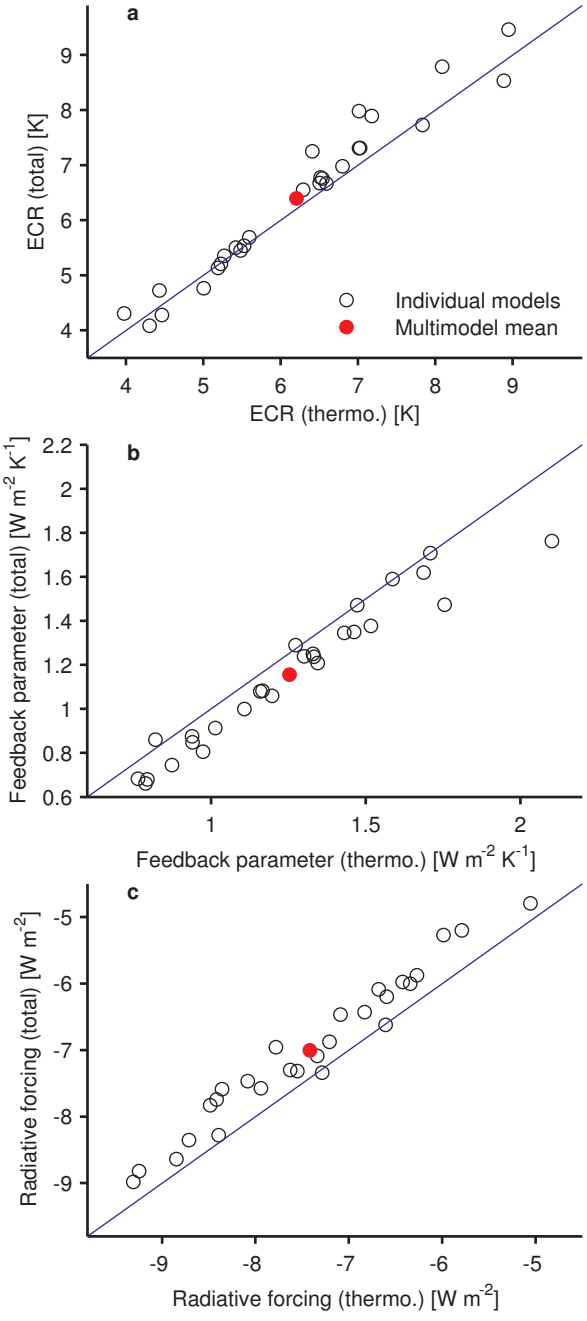

FIG. 7. Scatterplots of the (a) Equilibrium Climate Response (ECR), (b) global feedback parameter, and (c) radiative forcing for individual climate models (black open circles) and for the multimodel mean (red solid circles) in simulations subjected to an abrupt CO_2 quadrupling. The three quantities are calculated using the method of Gregory et al. (2004). The *y*-axes show the three quantities calculated using the total TOA all-sky radiative anomalies, and the *x*-axes show the quantities calculated using only the thermodynamic component of the total radiative anomalies. Hence, any departures from the one-to-one lines are due to changes in the large-scale atmospheric circulation.

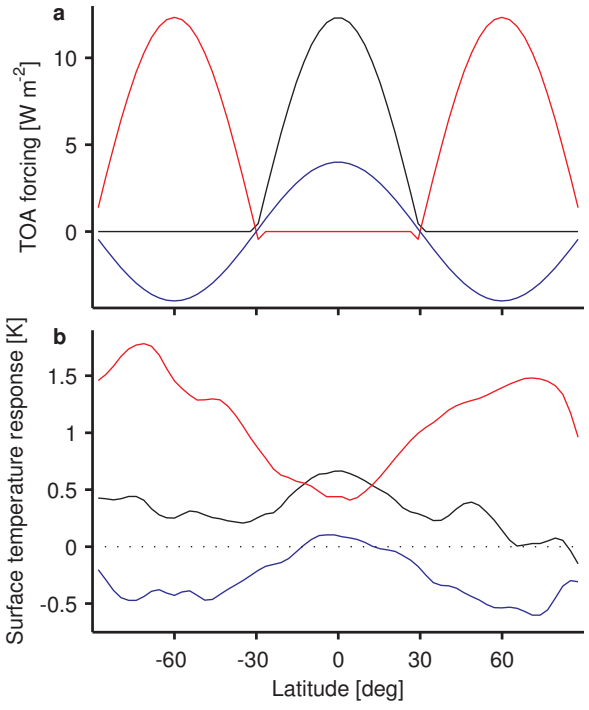

720 FIG. 8. (a) Imposed longwave TOA forcings (positive means heating) as a function of latitude for three
721 idealized simulations perturbed from the control run, and (b) the surface temperature response for each perturbed
722 simulation relative to the control run. The black lines correspond to the tropical forcing, the red lines to the
723 extratropical forcing, and the blue lines to the global-wave forcing. Each forcing has a $\cos 3\phi$ functional form.